Caspase-1 in *Cx3cr1*-expressing cells drives an IL-18-dependent T cell response that promotes parasite control during acute *T. gondii* infection

Isaac W. Babcock[1], Lydia A. Sibley[1], Sydney A. Labuzan[1], Maureen N. Cowan[1], Ish Sethi[1], Seblework Alemu[1], Michael A. Kovacs[1], John R. Lukens[1], and Tajie H. Harris[1]

Affiliations: [1]Center for Brain Immunology and Glia, Department of Neuroscience, University of Virginia, Charlottesville, VA 22908

Short title: Mechanisms of caspase-1-mediated immunity to acute *Toxoplasma gondii* infection

Corresponding Author and Lead Contact:
Tajie H. Harris
409 Lane Road, MR-4 Room 6148
Charlottesville, VA 22908
Phone: 434-982-6916
Email: tajieharris@virginia.edu

This work was funded by National Institute of Health grants R01NS112516 and R21NS128551 to T.H.H. and T32AI007496 to I.W.B. and 5T32GM136615 to L.A.S. and 5T32NS1156573 S.A.L. and a Pinn Scholars Award from the University of Virginia to T.H.H.

The authors have no financial or personal conflicts of interest to declare.

ABSTRACT

Inflammasome activation is a robust innate immune mechanism that promotes inflammatory responses through the release of alarmins and leaderless cytokines, including IL-1α, IL-1β, and IL-18. Various stimuli, including infectious agents and cellular stress, cause inflammasomes to assemble and activate caspase-1. Then, caspase-1 cleaves targets that lead to pore formation and leaderless cytokine activation and release. *Toxoplasma gondii* has been shown to promote inflammasome formation, but the cell types utilizing caspase-1 and the downstream effects on immunological outcomes during acute *in vivo* infection have not been explored. Here, using knockout mice, we examine the role of caspase-1 responses during acute *T. gondii* infection globally and in *Cx3cr1*-positive populations. We provide *in vivo* evidence that caspase-1 expression is critical for, IL-18 release, optimal interferon-γ (IFN-γ) production, monocyte and neutrophil recruitment to the site of infection, and parasite control. Specifically, we find that caspase-1 expression in *Cx3cr1*-positive cells drives IL-18 release, which potentiates $CD4^+$ T cell IFN-γ production and parasite control. Notably, our *Cx3cr1-Casp1* knockouts exhibited a selective T cell defect, mirroring the phenotype observed in *Il18* knockouts. In further support of this finding, treatment of *Cx3cr1-Casp1* knockout mice with recombinant IL-18 restored $CD4^+$ T cell IFN-γ responses and parasite control. Additionally, we show that neutrophil recruitment is dependent on IL-1 receptor accessory protein (IL-1RAP) signaling but is dispensable for parasite control. Overall, these experiments highlight the multifaceted role of caspase-1 in multiple cell populations contributing to specific pathways that collectively contribute to caspase-1 dependent immunity to *T. gondii*.

AUTHOR SUMMARY

When a cell undergoes inflammatory cell death, termed pyroptosis, cellular content is released and has the potential to stimulate immune responses. Our work highlights that in the context of *T. gondii* infection, distinct cell populations undergo pyroptosis each of which has different impacts on how the immune system responds. These findings suggest a collaborative effort of multiple cell types undergoing pyroptosis for optimal immunity to infection. Using a cell-type specific knockout to render macrophages incapable of undergoing pyroptosis, we find that macrophage pyroptosis reinforces adaptive immune cell function, while other population's pyroptosis stimulates the recruitment of innate immune cells into the infected tissue. We go on to identify a specific molecule, IL-18, is released from macrophage pyroptosis that reinforces adaptive immune cell function. By reintroducing IL-18 into the macrophage knockout mice, we successfully restored adaptive immune cell function thereby facilitating the recovery of parasite control. This study outlines the impact of pyroptosis on immunity to *T. gondii* and stratifies the effects from separate cell populations and their associated downstream pathways.

INTRODUCTION

Innate pathogen sensing via pattern recognition receptors (PRRs) instructs and mobilizes the immune system in response to infections. The diversity of PRRs and the molecules they recognize tailor the immune response generated. These PRRs include toll-like receptors (TLR), Nod-like receptors (NLR), and C-type lectin receptors (1). Specifically, activation of some NLRs triggers the formation of a multi-protein complex known as the inflammasome. The effector protein of the inflammasome is caspase-1, which cleaves substrates including those that create pores in the cell membrane. Consequently, this process prompts inflammatory cell death and the release of immune-activating cytosolic contents, including leaderless cytokines which do not leave the cell through conventional secretion pathways and rely on proteolytic cleavage for activation (2, 3). Currently, it remains unclear how inflammasome activation is orchestrated across cell types during an infection and whether each cell type has the same ability to activate the inflammasome and release inflammatory cargo. To investigate this question, we employed an *in vivo* mouse model of *Toxoplasma gondii* infection, in which the activation of the inflammasome has been reported to result in the release of various immunostimulatory molecules.

T. gondii is an obligate intracellular parasite that can infect nearly all nucleated cells. The parasite replicates throughout the body of the host during the acute phase of infection and then resides in the brain for the duration of the host's life as a chronic infection. Host survival depends on the adaptive immune system's ability to produce interferon gamma (IFN-γ) (4-7). IFN-γ signaling stimulates the expression and production of proteins that facilitate intracellular pathogen-killing mechanisms, enabling the control of the parasite (8-10). The dependence on IFN-γ underscores the vital role of innate immune sensing, which initiates production of cytokines like IL-12 and IL-18 that bridge the innate the adaptive immune system. In mice, TLR11/12 molecules on dendritic cells

recognize *T. gondii* profilin resulting in MyD88-dependent IL-12 release (11-14). IL-12 acts on natural killer (NK) and T lymphocyte cells to promote an IFN-γ response (15-17). Of note, humans lack functional TLR11/12 and can still mount an effective immune response to *T. gondii*, suggesting that other innate sensors recognize and respond to the parasite. One such sensor is the inflammasome, which has been suggested to promote protective immunity during acute infection in humans, rats, and mice (18-22). At present, *in vitro* studies and survival studies have been performed but which cells utilize caspase-1 at various stages of *T. gondii* infection and the immunological consequences have not been defined.

The inflammasome mediates the release of cytoplasmic cytokines (leaderless cytokines) and premade immunostimulatory molecules (alarmins). *In vitro* and *in vivo* studies have shown that *T. gondii* infection promotes the release of leaderless cytokines IL-1α, IL-1β, IL-33, and IL-18 and the alarmin s100a11 (18, 19, 21, 23-28). A recent study by López-Yglesias, et. al demonstrated that in the absence of TLR11, inflammasome effector proteins caspase-1/11 promote $CD4^+$ T cell IFN-γ production (20). Another study observed that enhancing IL-18's ability to bind cell surface receptors can promote stronger $CD4^+$ T cell and NK cell IFN-γ production during *T. gondii* infection (29). Additionally, it was reported that during acute infection IL-1 signaling onto its cognate receptor IL-1R is required for neutrophil recruitment to the site of infection, but this signal was dispensable for IFN-γ responses (24). Furthermore, during acute infection, the alarmin s100a11 promotes a *Ccl2*-mediated monocyte recruitment to the site of infection. Together, these studies indicate that caspase-1/11 may play a role in multiple facets of the immune response to *T. gondii*. However, it remains uncertain whether caspase-1 specifically is necessary and whether caspase-1 in distinct cell types performs specific roles in inflammasome activity or if a single population is responsible for the release of multiple leaderless cytokines and alarmins.

To investigate caspase-1-mediated immunity against *T. gondii*, we used whole-body and cell-type-specific knockout mice. Using this approach, we report that caspase-1 is required for optimal parasite control, promoting $CD4^+$ T cell IFN-γ production and enhancing neutrophil and monocyte recruitment to the initial site of infection. In particular, we find that *Cx3cr1*-positive cells use caspase-1 to release IL-18, which reinforces IFN-γ production. On the other hand, monocyte and neutrophil responses were intact in these mice, which suggests that caspase-1 activity in additional cell types regulates these innate responses. Our studies demonstrate that in the context of *in vivo T. gondii* infection caspase-1 is utilized in distinct cell populations to carry out non-overlapping and specific downstream effects of caspase-1-mediated immunity to *T. gondii.*

RESULTS

Caspase-1 mediates aspects of innate and adaptive immunity to T. gondii.

The initial studies examining the role of inflammasomes in *T. gondii* infection were performed in double knockout mice, in which expression of both *Casp1* and *-11* were ablated and immunity against the parasite was impaired (18-20). We hypothesized that the caspase-1 canonical inflammasome pathway would be sufficient to drive multiple aspects of protective immunity towards *T. gondii*. Therefore, we infected *Casp1* single knockout mice with 10 cysts of Me49 type II strain parasite by intraperitoneal (i.p.) infection (30). Then, we performed peritoneal lavage at eight days post-infection (8 dpi) and found that the parasite burden was 3.6-fold greater in *Casp1* deficient mice compared to WT controls (Fig 1a). Additionally, during chronic infection at six

weeks post-infection (6 wpi), we found a 1.4-fold increase in parasite burden in the brains of *Casp1* KO mice relative to control mice (S1a Fig). Surprisingly, *Casp1* and *Casp1/11* KO mice had similar long-term survival post-infection compared to WT mice (S1b Fig), but consistently had higher parasite burdens. To test if the increased parasite burden at day 8 was due to an immunological defect, we performed ELISAs on the serum of WT and *Casp1* KO mice. We found that *Casp1* KO mice had a 25% reduction in IFN-γ levels compared to WT controls (Fig 1b) but had comparable IL-12 serum levels (Fig 1c). On the other hand, we found that IL-18 serum levels in *Casp1* KO mice were nearly half of what was measured in WT controls (Fig 1d). We were unable to detect IL-1α or IL-1β in the serum at this timepoint, consistent with prior reports (19, 20, 31).

As IFN-γ is a major regulator of immunity to *T. gondii*, we then aimed to identify cell populations where IFN-γ production was impacted by *Casp1* deficiency. We harvested spleen and peritoneal exudate cells at 8 days post-infection and used spectral flow cytometry to identify IFN-γ-producing cell populations. We found fewer $CD4^+$ T cells that produced IFN-γ within the spleen in *Casp1* KO mice in comparison to WT controls (Fig 1d-f). *Casp1* was dispensable for splenic $CD8^+$ T cells, NK cells, and ICL1/NK T cells IFN-γ production (S1c-S1e Fig). Additionally, in the peritoneum 8 dpi, no consistent defect was seen in IFN-γ production by $CD4^+$ and $CD8^+$ T cells or by NK/ ILC1 and NK T cells (S1f-S1i Fig). Together these data highlight a defect in IFN-γ production specific to splenic $CD4^+$ T cells in mice lacking *Casp1*.

Beyond a defect in IFN-γ production, we observed a dramatic decrease in the number of neutrophils ($CD11b^+Ly6G^+$) and monocytes ($CD11b^+$ $Ly6G^-$ $Ly6C^+$) recruited to the peritoneum

153 in *Casp1* KO mice compared to WT mice (Fig 1h-l). Corresponding to the decreased monocyte
154 infiltration, in the peritoneum we found decreased levels of the mRNA for the monocyte
155 chemoattractant, Ccl2, in the peritoneum of *Casp1* KO mice compared to WT (Fig 1j). Similarly,
156 mRNA levels of Cxcl1 and Cxcl2, major chemokines for neutrophil attraction, were decreased in
157 whole-body *Casp1* KO peritoneal lavage fluid (Fig 1m). Together these data demonstrate that
158 *Casp1* deficiency leads to innate and adaptive immune defects that are associated with an inability
159 to fully control parasite levels during acute *T. gondii* infection.
160
161 *IL-18 promotes CD4$^+$ T cell IFN-γ production but is dispensable for myeloid cell recruitment to*
162 *the initial site of infection.*
163
164 We hypothesized that the decreased IL-18 serum levels in whole-body *Casp1* knockout mice
165 impaired CD4$^+$ T cell IFN-γ production. Thus, we infected *Il18* KO and WT control mice to gain
166 insight on which immune responses downstream of caspase-1 activation were dependent on IL-
167 18. Mice were infected with 10 cysts Me49 followed by analysis of peritoneal exudate cells and
168 spleens at eight days post-infection. Similar to *Casp1* deficient mice, *Il18* deficient mice displayed
169 an increased parasite burden in the peritoneal cavity and decreased serum IFN-γ levels (Fig 2a and
170 Fig2b). Likewise, *Il18* deficiency had no effect on serum IL-12 levels (Fig 2c). In the spleens of
171 *Il18* deficient mice, IFN-γ production by CD4$^+$ T cells was impaired (Fig 2d-f), but IFN-γ
172 production by CD8$^+$ T cells was unimpaired (S2a Fig). In the peritoneal cavity of *Il18* KO mice a
173 defect in IFN-γ production by CD4$^+$ and CD8$^+$ T cells was also observed (S2b-d Fig). These data
174 suggest that IL-18 promotes CD4$^+$ T cell IFN-γ production during the acute phase of *T. gondii*
175 infection and is consistent with results observed in *Casp1* deficient mice. On the other hand, when

we assayed myeloid cell responses in the peritoneum, neutrophil and monocyte numbers were comparable between *Il18* deficient and WT controls (Fig 2g-j). Together, these results suggest that IL-18 is essential for full parasite control and likely represents one arm of the caspase-1-dependent immune response during the acute stage of *T. gondii* infection.

Given the specificity of the IL-18 response, we next examined IL-18 receptor (IL-18R) expression to begin to understand why IFN-γ production is specifically impaired in splenic $CD4^+$ T cells in *Il18*-deficient mice at day 8 post-infection. We quantified IL-18R-positive $CD4^+$ and $CD8^+$ T cells in the spleen and peritoneal cavity at 8 days post-infection (S2e Fig). Approximately 30% of $CD4^+$ T cells in the spleen and nearly 80% of $CD4^+$ T cells in the peritoneum expressed IL-18R, while only a small fraction of $CD8^+$ T cells expressed the receptor (S2f Fig). To understand if IL-18R expression on T cells is infection-dependent, we compared IL-18R expression between naïve and infected mice. We found that few splenic T cells express IL-18R at baseline (S2g Fig). These data suggest that $CD4^+$ T cells are more responsive to IL-18, due to infection-induced upregulation of IL-18R.

IL-1Rap mediates neutrophil recruitment but is dispensable for parasite control at the site of infection.

IL-18 is one of many molecules that can be released downstream of caspase-1. To broadly test if the loss of other leaderless cytokine signaling could recapitulate whole-body capase-1 deficiency during acute *T. gondii* infection, we utilized *IL-1 receptor accessory protein (Il1rap)* knockout mice. IL-1RAP is a necessary receptor subunit for IL-1, IL-33, and IL-36 receptor signaling. We infected *Il1rap* WT and KO mice with 10 cysts Me49 and performed peritoneal lavage at eight

days post infection. We observed no difference in parasite burden between *Il1rap* KO and WT control mice at this site (Fig 3a). Furthermore, we observed no difference in IFN-γ serum levels or splenic $CD4^+$ T cell IFN-γ production (Fig 3b-d). In the peritoneum, *Il1rap* KO mice had comparable monocyte responses (Fig 3e-g). However, there was a severe impairment in neutrophil recruitment to the site of infection in *Il1rap* KO mice (Fig 3h-j). These results are in line with a previous report showing that IL-1R signaling is required for neutrophil recruitment during acute infection and is dispensable for IFN-γ responses (24). Taken together, these data suggest that IL-1RAP signaling is critical for neutrophil responses but is dispensable for parasite control in the presence of IFN-γ and monocytes.

Caspase-1 in Cx3cr1-expressing cells is necessary for parasite control and optimal production of IFN-γ by $CD4^+$ T cells

To begin to address how caspase-1 activation shapes immunity to *T. gondii*, we sought to identify which cells type(s) are involved. We aimed to identify the population responsible for caspase-1-mediated IFN-γ production and parasite control. To this end, we utilized a single-cell RNA sequencing dataset that examined gene expression in the spleen at day 14 post-infection with *T. gondii*. We focused on cell types that express IL-18, as the release of this cytokine is significantly decreased in *Casp1* deficient mice. At this timepoint, we confirmed that macrophages are a major source of *Il18* and *Casp1* expression (S3a-S3b Fig). We hypothesized that caspase-1 activity in macrophages would be necessary for parasite control, optimal cytokine production, and cellular recruitment to the peritoneal cavity. To test this hypothesis, we crossed mice that constitutively express cre recombinase under the *Cx3cr1* promoter to a *Caspase*-$1^{fl/fl}$ background (32, 33). We

222 infected *Cx3cr1*$^{cre/+}$ x *Caspase* 1$^{fl/fl}$ and *Cx3cr1*$^{+/+}$ x *Caspase* 1$^{fl/fl}$ littermate controls with 10 cysts
223 Me49 and at eight days post infection we harvested tissues. For simplicity, we have abbreviated
224 *Cx3cr1*$^{cre/+}$ x *Caspase* 1$^{fl/fl}$ as macrophage (MΦ) *Casp1* KO, given that macrophages represent a
225 large portion of the *Cx3cr1*$^{+}$ population (32, 34). In the peritoneum, we saw a ~3-fold increase in
226 parasite burden in the macrophage *Casp1* KO mice compared to control mice (Fig 4a), which was
227 associated with a greater cyst burden in the brains of these mice at 6 weeks post-infection (6wpi)
228 (S3c Fig). At day eight post-infection, we performed ELISAs on the serum and found that
229 macrophage *Casp1* KO mice had decreased IFN-γ levels, comparable IL-12 levels, and decreased
230 IL-18 levels compared to WT mice (Fig 4b-d). These data suggest that a *Cx3Cr1*$^{+}$ cell population
231 promotes IL-18 release and enhances IFN-γ production. Using spectral cytometry, we found that
232 macrophage *Casp1* KO mice had impaired production of IFN-γ in splenic CD4^{+} T cells (Fig 4e-
233 g). IFN-γ production by splenic CD8^{+} T cell was unimpaired, as was IFN-γ production by
234 peritoneal CD4^{+} and CD8^{+} T cells (S3b-S3d Fig). When we examined neutrophil and monocyte
235 recruitment to the peritoneal cavity, both responses were intact and comparable to WT levels (Fig
236 4h-m). These data show that macrophage *Casp1* KO mice exhibited a selective T cell defect are
237 nearly identical in phenotype to the *Il18* knockout mice.
238
239 *Recombinant IL-18 administration rescues CD4*$^{+}$ *T cell IFN-γ production and parasite control in*
240 *macrophage caspase-1 deficient mice.*
241
242 Macrophage *Casp1* KO mice had decreased serum IL-18 levels and phenocopied *IL-18* KO mice
243 with both having selective impairment in CD4^{+} T cell IFN-γ production. Thus, we hypothesized
244 that the decreased IL-18 levels in macrophage *Casp1* KO mice leads to decreased CD4^{+} T cell

IFN-γ production and parasite control. To test this hypothesis, we performed a rescue experiment, where we administered recombinant IL-18 (rIL-18) at 10μg/kg or PBS to macrophage *Casp1* deficient mice at 1 hour post-infection and on days 1, 3, 5, and 7 post-infection (Fig 5a). We confirmed that the rIL-18 treatment restored IL-18 serum levels (Fig 5b). As expected, parasite burden was greater in macrophage *Casp1* KO mice that received PBS treatment compared to WT controls. However, in macrophage *Casp1* KO mice that received rIL-18, parasite burden was comparable to levels seen in WT mice (Fig 5c). Furthermore, we found that rIL-18 treatment was able to rescue IFN-γ serum levels while leaving IL-12 levels unchanged (Fig 5d and Fig 5e). Together, these data demonstrate that administering rIL-18 in macrophage *Casp1* KO mice was sufficient to restore IFN-γ production and ultimately recuperate parasitic control. We hypothesized that the recovery of IFN-γ serum levels in mice that received rIL-18 administration would coincide with a recovery in frequency and number of splenic $CD4^+$ T cells making IFN-γ. Indeed, when flow cytometry was performed on splenic cells at 8 dpi, we found that rIL-18 was able to restore IFN-γ production to splenic $CD4^+$ T cells in macrophage *Casp1* KO mice (Fig 5f-h). Thus, administration of rIL-18 was sufficient to rescue $CD4^+$ T cell IFN-γ production and parasite control in mice lacking caspase-1 production in *Cx3cr1*$^+$ expressing cells. Taken together, these results highlight the importance of caspase-1 in *Cx3cr1*-positive populations to promote IL-18 release. These studies demonstrate the varied contributions of caspase-1-mediated pathways during an infection. One arm of the caspase-1 response mediates IL-18 release to impact T cell cytokine production and pathogen control, while other arms stimulate signaling (including through IL-1RAP), to mediate cellular recruitment to the site of infection.

DISCUSSION

Prior studies on caspase-1/11 during *T. gondii* infection have revealed the capacity of inflammasomes to release various molecules *in vivo* and *in vitro* (18-20, 23, 35). However, prior to the current study, the necessity of caspase-1 rather than caspase1/11 and the specific cell types utilizing caspase-1 and the immunological responses triggered by caspase-1 activity *in vivo* were unknown. Traditionally, studies on caspase-1 have employed *in vitro* cultures utilizing a single cell type. The development of caspase-$1^{fl/fl}$ mice has allowed for a more detailed exploration of caspase-1 activity *in vivo* (33). This study presents evidence indicating that distinct cell populations use caspase-1 to support different facets of immunity to *T. gondii*. Specifically, *Cx3cr1*-positive populations utilize caspase-1 to promote IL-18 release, which facilitates $CD4^+$ T cell IFN-γ production. In contrast, another population(s) leverages caspase-1 for neutrophil recruitment through IL-1RAP signaling and monocyte recruitment via induction of the chemokine CCL2.

We identified a caspase-1/IL-1RAP signaling axis as a necessary component of neutrophil recruitment to the site of infection. The role of neutrophils during acute *T. gondii* has been an active area of investigation. A previous report using an anti-Gr-1 antibody to deplete neutrophils suggests that neutrophils are critical for parasite control (36). Anti-Gr-1 is not specific to neutrophils and results in the depletion of inflammatory monocytes, making it difficult to interpret the importance of neutrophils during acute *T. gondii* infection. Interestingly, a recent *in vitro* study showed that *T. gondii*-induced neutrophil extracellular trap (NET) formation promoted the migration and cytokine response of T cells, suggesting that neutrophils can promote a more robust adaptive immune response (37). A third study using an antibody targeting Ly6G to obtain a more selective depletion of neutrophils found no role for neutrophils in parasite control or IFN-γ levels in orally infected

mice (38). Similarly, our study using *Il1rap* KO mice which only had a defect in neutrophil recruitment to the site of infection suggests that neutrophils are not necessary for *T. gondii* control or IFN-γ production. Interestingly, both IL-33 signaling (ST2) and IL-1 signaling (IL-1R1) utilize IL-1RAP and have been associated with neutrophil recruitment during acute *T. gondii* infection (24, 39). In both of these studies the knockout of each respective receptor brought neutrophil levels drastically down. Thus, although neutrophil recruitment is regulated through caspase-1 and IL-1RAP signaling, this specific immunological response to *T. gondii* appears to be dispensable for parasite control and is in agreement with studies that used anti-Ly6G antibodies to deplete neutrophils. Whether caspase-1 mediates the release of IL-33, IL-1β, and/or IL-1α to promote neutrophil recruitment remains unresolved. Caspase-1 cleavage of IL-33 is suggested to inactive the cytokine (40) but the mechanism of IL-33 release is still under investigation (41). Recent studies have identified that IL-33 is released from cells via gasdermin D pore formation, but the protease activating gasdermin D varied with the stimulus used to induce IL-33 release (42, 43). Thus, whether caspase-1 liberates IL-33 or inactivates IL-33 during *T. gondii* infection is of interest.

Our study on *Il1rap* KO mice not only provided insight the role of neutrophils during *T. gondii* infection but also on monocyte recruitment. As both *Il18* KO and *Il1rap* KO mice had no defect in monocyte recruitment, our data suggests an additional signal is promoting monocyte recruitment to the site of *T. gondii* infection. Our study aligns with a recent report describing how monocytes are recruited to the site of infection. Specifically, Safronova, et al. recently described that the alarmin S100a11 mediates *Ccl2* expression and monocyte recruitment to the peritoneal cavity following infection. In accordance, they found that S100a11 release was caspase-1/11-dependent,

both *in vitro* and *in vivo* (23). Together with our study, this suggests that a population (s) other than macrophages is driving caspase-1/S100a11-/CCL2-dependent monocyte recruitment.

Our study is also in accordance with a recent study from Clark et. al., which describes that IL-18 and its regulation impacts the ability of $CD4^+$ T cells to make IFN-γ (29). Although, initially we were surprised to see that the NK cell IFN-γ response is intact in *Casp1* and *Il18* KO mice, López-Yglesias, et. al. also showed that *Casp1/11* deficiency had no impact on NK cell IFN-γ responses. One likely explanation is that the timing of IL-18 interaction with NK cells is critical. It has been observed that if an NK cell interacts with IL-12 before interacting with IL-18, IL-18 will not impact NK cell IFN-γ production (44). During *T. gondii* infection IL-12 levels are detected and increase before IL-18 levels (45-47), thus NK cells may encounter IL-12 well before IL-18, explaining why IL-18 has minimal impact on NK cell activation. We were also surprised by the specificity of the IFN-γ defects in splenic $CD4^+$ T cells and not $CD8^+$ T cells in *Casp1*, *Il18*, and macrophage *Casp1* knockouts. These results can be explained by the preferential upregulation of IL-18R on $CD4^+$ T cells at day 8 post-infection. Interestingly, the report by Clark et. al. demonstrates that $CD8^+$ T cells upregulate IL-18R expression at day 10 post-infection (29). Thus, the expression of IL-18R on $CD8^+$ T cells is tightly regulated by an unknown cue. Similarly, we found that NK cell/ILC1 cell population expression of IL-18R is absent at baseline and present at day eight post-infection, whereas, in accordance with Clark et. al., the NK T cell population expressed IL-18R at baseline and at day eight (29). Interestingly, our study and the study from Clark et. al. showed that exogenous addition of IL-18 did not impact NK cell IFN-γ production, but Clark et. al. showed that when a recombinant IL-18 resistant to inhibition by IL-18 binding protein was exogenously added, NK cell responses and IFN-γ production were enhanced. These data suggest that the

337 response of NK cells to IL-18 is highly regulated. Overall, these data suggest that IL-18 release
338 and IL-18R expression are exquisitely controlled and ultimately influence the quality of $CD4^+$ T
339 cell production of IFN-γ.
340
341 While the current study has identified the importance of caspase-1 activity in specific cell
342 populations, the signal(s) that leads to inflammasome activation remain unclear. Additionally, as
343 multiple inflammasome sensors have shown to be triggered by *T. gondii*, it is possible that in the
344 *Cx3cr1*-positive and other populations, caspase-1 is activated by distinct mechanisms and sensors.
345 *In vitro*, both direct *T. gondii* infection and extracellular signaling cascades have been proposed to
346 initiate the inflammasome (18, 27, 48, 49). Cell-intrinsic signals and cellular stress are also
347 possible modes of inflammasome activation (50, 51). Although, during *in vivo T. gondii* infection,
348 it is unclear whether direct invasion of the parasite and/or an infection-associated trigger is
349 necessary for caspase-1 activation. A recent study by Wang, et. al., identified that in bone marrow
350 derived macrophages (BMDMs) from the Lewis rat, NLRP1-dependent pyroptosis is mediated by
351 direct infection and three parasite dense granule proteins GRA35, 42, and 43 (27). In the human
352 monocyte cell line (THP-1) cell cultures infected with *T. gondii*, the AIM2 inflammasome sensor
353 has been shown to be activated by *T. gondii* DNA that has been liberated by guanylate binding
354 protein (GBP) activity (48, 52). A third study using primary mouse peritoneal macrophages and
355 BMDMs identified that NLRP3 was activated by extracellular ATP signaling released from
356 parasite infected cells (49). Our data along with these *in vitro* experiments raise the question of
357 whether certain cell types can activate multiple inflammasome sensors and release multiple
358 leaderless cytokines or DAMPs. In the single cell data set we analyzed, the splenic macrophage
359 population containing IL-18 expressed AIM2 more than other inflammasome sensors (29). We did

not observe prominent expression of NLRP3 within the splenic macrophage population which is consistent with work from López-Yglesias et. al., which showed that NLRP3 does not impact $CD4^+$ T cell IFN-γ production during acute *T. gondii* infection (20). NLRP1 which has been shown to confer resistance to *T. gondii* infection in humans and rats (18, 21, 35) and has been reported to modulate IL-18 release in mice (19), was expressed in only a small percentage of splenic IL-18-expressing cells. Ultimately, whether one sensor or multiple sensors contribute to the distinct caspase-1 activities remains an open question.

In addition, the responses downstream of inflammasome activity are influenced by cellular expression of leaderless cytokines, leaderless cytokine receptors, and the chemokines a receptive cell can produce. Furthermore, the spatial location of these interactions likely influences the effects of inflammasome activity. For instance, IL-1α and IL-1β are regulated by a soluble receptor antagonist (IL-1R antagonist) which competes with surface receptors. Thus, efficient IL-1 signaling may require local proximity of a IL-1R1-expressing cell (53). Similarly, IL-18 is regulated by IL-18BP, making the proximity of IL-18 release near responding $CD4^+$ T cells critical for optimal IFN-γ production. To parse out this complex and specific interplay, high-dimensional spatially-resolved data sets will be of value. In this study, we were able to use a previously published single-cell RNA sequencing dataset to aid in the identification of a putative cell population capable of activating caspase-1 and releasing IL-18. The use of spatial transcriptomics and its ability to identify cells harboring leaderless cytokines and identify proximal cells able to respond to the cytokine will be advantageous for future studies on the orchestration of local inflammasome responses. The current study also demonstrates that distinct cell types use caspase-1 to impact innate and adaptive immune responses, which may provide an advantage to the host.

383 The separation of the potent effects of caspase-1 activity across multiple cell types with differential
384 inflammasome activation capacity likely acts as a checkpoint to prevent excess inflammation.
385 Having a layered regulation of inflammasome activation *in vivo* allows for a broad range of
386 activators to elicit specific and non-redundant responses.
387
388 As our study focused on the role of caspase-1 during acute *T. gondii* infection, it is unclear if a
389 similar paradigm of cell-type specificity occurs in the brain during chronic *T. gondii* infection. As
390 the brain contains long-lived cells which do not regenerate, the control of inflammation in this
391 tissue is critical. A layered regulation of caspase-1 activity in the CNS would be advantageous for
392 controlling *T. gondii* without promoting excess deleterious inflammation. A recent study by our
393 group (24) identified that microglia, a *Cx3cr1*-positive cell population, releases IL-1α to promote
394 myeloid cell recruitment into the infected brain and control parasite. This contrasts with acute
395 infection where a population(s) other than *Cx3cr1*-positive cells contributes to myeloid
396 recruitment. This highlights a significant difference in caspase-1 biology in the infected CNS and
397 raises the important question of whether the CNS contains multiple cell types capable of activating
398 caspase-1 to carry out unique aspects of immunity. Given that *Casp1* and *Casp1/11* deficient mice
399 have higher parasite burdens in the CNS, it suggests that inflammasome activity is necessary in
400 the brain and likely regulates local immune responses.
401

402 **METHODS**

403 **Animals and Infection**

404 WT (C57BL/6J), *Caspase-1*$^{-/-}$ (#32662) (30), *Caspase1/11*$^{-/-}$ (#016621) (54), *Cx3Cr1*$^{cre/cre}$
405 (#025524) (32), *Il18*$^{-/-}$ (#004130) (55) and *Il1rap*$^{-/-}$(#003284) (56) strains were obtained from

406 The Jackson Laboratory and maintained within our animal facility. Caspase-1$^{fl/fl}$ mice were
407 provided by R. Flavell (33). *Cx3Cr1*$^{cre/cre}$ mice were cross-bred with Caspase-1$^{fl/fl}$ mice to generate
408 *Cx3Cr1*$^{cre/+}$ x Caspase-1$^{fl/fl}$. The type II *T. gondii* strain Me49 was maintained in Swiss Webster
409 mice (#024, Charles River Laboratories) and passaged through CBA/J mice (Jackson Laboratory).
410 For experiments, tissue cysts were collected from chronically infected (>4 weeks) CBA/J mice. 7–
411 10-week-old age and sex-matched mice were injected intraperitoneally with 10 cysts of Me49 in
412 200 µL of 1X PBS. Sham-infected mice were injected with an equal volume of 1X PBS. For rIL-
413 18 experiments, 10 µg/kg or PBS of equivalent volume was given to mice on day 0, 1, 3, 5, and 7
414 post-infection with *T. gondii*. Mice used for endpoint studies were euthanized if they showed
415 weight loss greater than 20% of their pre-infection bodyweight. All procedures involving animal
416 care and use were approved by and conducted in accordance with the University of Virginia's
417 Institutional Animal Care and Use Committee (IACUC) under protocol number 3968.

418

419 ***T. gondii* qPCR**

420 Parasite genomic DNA was isolated from mouse peritoneal exudate cells and whole brain using
421 the Isolate II Genomic DNA Kit (Bioline, BIO-52067). Prior to isolation, brain was first
422 homogenized in 1X PBS using the Omni TH tissue homogenizer (Omni International).
423 Amplification of *T. gondii* 529 bp repeat region using the SensiFAST Probe No-ROX Kit (Bioline,
424 BIO-86005) and CFX384 Real-Time System (Bio-Rad) was performed as previously described
425 (57) Tissue DNA (500 ng or 1µg) was loaded into each reaction. *T. gondii* isolated from human
426 foreskin fibroblasts was used to make a serial standard curve from 3 to 300,000 genome copies
427 and determine the number of *T. gondii* genomes per µg of tissue DNA.

Tissue processing

Immediately after sacrifice a peritoneal lavage was performed with 3 mL of 1X PBS. Peritoneal material was pelleted, resuspended in 700 µL complete RPMI media (cRPMI; 10% FBS [Gibco], 1% penicillin/streptomycin [Gibco], 1% sodium pyruvate [Gibco], 1% non-essential amino acids [Gibco], and 0.1% 2-Mercaptoethanol [Life Technologies]). Subsequently, blood was collected from the superior vena cava, allowed to clot, and then spun down at 15 x *g* for 25 minutes. Serum was collected and stored at -70° C until further use. Then, transcardiac perfusion with 20 mL cold 1X PBS was performed. Spleens were taken and placed in 2 mL complete RPMI media. Spleens were then mechanically passed through a 40 µm filter (Corning, Ref 352340), spun down at 6,000 rpm for 3 min, and resuspended in red blood cell lysis buffer (0.16 M NH_4Cl) for 2 minutes. The cells were then washed with cRPMI, pelleted, and resuspended in 5 mL cRPMI. For intracellular cytokine staining, cells were resuspended in 50 µL cRPMI with Brefeldin A (Selleckchem Cat#S7046) for 5 hours at 37° C before staining.

Flow cytometry

For myeloid cell panels, single cell suspensions were resuspended in Fc Block, made in FACS buffer (1X PBS, 0.2% BSA, and 2 mM EDTA) with 0.1 µg/ml 2.4G2 Ab (BioXCell, Cat#CUS-HB-197) and 0.1% rat gamma globulin (Jackson Immunoresearch, Cat#012-000-002) for 10 minutes. Cells were stained for surface markers and eBioscience fixable live/dead viability dye efluor506 (1:800 Cat#65-0866-14) for 30 min at 4° C. Cells were then washed twice with 100 µL FACS buffer. For intracellular staining, cells were fixed with fixation/permeabilization solution

(eBioscience, 00-5123-43 and 00-5223-56) for 15 min at room temperature. Cells were then washed twice with 100 µL permeabilization buffer (eBioscience, 00-8333-56) and stained for intracellular markers in 1X perm buffer for 20 min at 4° C and subsequently washed with 1X perm buffer. Finally, cells were resuspended in 200 µL FACS buffer and acquired using a 3 laser Cytek Aurora Flow Cytometry System. Data was analyzed using FlowJo software v10.9.0. For myeloid panels the following antibodies at 1:200 were used: CD45-FITC (eBioscience, Cat#11-0451-82), CD11b-APC-efluor780 (eBioscience, Cat#47-0112-82), CD11c-PerCP-Cyanine5.5 (eBioscience, Cat#45-0114-82), iNOS-APC (eBioscience, Cat#17-5920-82), Ly6G-Pacific Blue (Stemcell Technologies, Cat#60031PB), Ly6C-Pe-Cy7 (Biolegend, Cat#128018). For T cell and cytokine panels the following antibodies at 1:200 were used: CD4-efluor450 (eBioscience, Cat#2114200), CD3-FITC (eBioscience, Cat#2159105), CD8α-PerCP-Cyanine5.5 (eBioscience, Cat#2410098), T-bet-PE-Cyanine7 (eBioscience, Cat#2410093), CD44-APC-efluor780 (eBioscience, Cat#2373711), IFN gamma-APC (eBioscience, Cat#2175632), CD218α (IL-18r)-PE (BioLegend, Cat#157903), CD62L-BV650 (BioLegend, Cat#104453), NK1.1-Super Bright 780 (eBioscience, Cat#78-5941-82).

ELISA

Serum cytokine levels were detected according to R&D systems instructions using either DuoSet ELISA kits (IFN-γ, Cat# DY485-05) (IL-18, Cat# DY7625-05) with the DuoSet Ancillary Reagent Kit 2 (Cat# DY008B) or Quantikine ELISA (IL-12, Cat#M1240).

RT-qPCR

Peritoneal exudate cells were homogenized in Trizol. RNA was extracted according to the manufacturer's (Invitrogen) protocol. cDNA was then generated using a High-Capacity Reverse Transcription Kit (Applied Biosystems). Quantitative PCR was performed using 2X Taq based Master Mix (Bioline) and Taq Man gene expression assays (Applied Biosystems). Samples were run on a CFX384 Real-Time System thermocycler (Bio-Rad Laboratories). Genes were normalized to murine *Hprt.* The $2^{(-\Delta\Delta CT)}$ method was used to report relative expression(58). The following ThermoFisher mouse gene probes were used: Hprt (Mm00446968_m1), *Ccl2* (Mm00441242_m1), *Cxcl1* (Mm04207460_m1), and *Cxcl2* (Mm00436450_m1).

Single cell sequencing analysis

The publicly available count matrix from GSE207173 (Clark et al., 2023) was imported into a Python environment and processed using Scanpy. For quality thresholds, cells with less than 1k counts, cells greater than 25k counts, or cells containing greater than 20% mitochondrial RNA content were filtered and excluded from the analysis. The data matrix was normalized and logarithmized, and PCA was used for dimensionality reduction using the ARPACK wrapper. Unsupervised clustering was performed using the leiden algorithm, with a resolution set to 0.6.

Statistical analysis

All data was graphed in GraphPad Prism 9. To account for the biological variability between infections, data from experiment replicates was analyzed in R using a randomized block ANOVA. This analysis models experimental groups as a fixed effect and experimental day as a random effect

493 (59). Outliers were identified and removed using ROUTs method with a Q value of 1 (60). *p*

494 values are indicated, with ns = not significant, $p < 0.05$ (*), $p < 0.01$ (**), and $p < 0.001$ (***).

REFERENCES

1. Takeuchi O, Akira S. Pattern Recognition Receptors and Inflammation. Cell. 2010;140(6):805-20.
2. Kanneganti TD, Lamkanfi M, Núñez G. Intracellular NOD-like receptors in host defense and disease. Immunity. 2007;27(4):549-59.
3. Kesavardhana S, Malireddi RKS, Kanneganti TD. Caspases in Cell Death, Inflammation, and Pyroptosis. Annu Rev Immunol. 2020;38:567-95.
4. Suzuki Y, Orellana MA, Schreiber RD, Remington JS. Interferon-gamma: the major mediator of resistance against Toxoplasma gondii. Science. 1988;240(4851):516-8.
5. Scharton-Kersten T, Contursi C, Masumi A, Sher A, Ozato K. Interferon consensus sequence binding protein-deficient mice display impaired resistance to intracellular infection due to a primary defect in interleukin 12 p40 induction. J Exp Med. 1997;186(9):1523-34.
6. Scharton-Kersten TM, Wynn TA, Denkers EY, Bala S, Grunvald E, Hieny S, et al. In the absence of endogenous IFN-gamma, mice develop unimpaired IL-12 responses to Toxoplasma gondii while failing to control acute infection. The Journal of Immunology. 1996;157(9):4045-54.
7. Gazzinelli RT, Hakim FT, Hieny S, Shearer GM, Sher A. Synergistic role of CD4+ and CD8+ T lymphocytes in IFN-gamma production and protective immunity induced by an attenuated Toxoplasma gondii vaccine. J Immunol. 1991;146(1):286-92.
8. Frickel EM, Hunter CA. Lessons from Toxoplasma: Host responses that mediate parasite control and the microbial effectors that subvert them. J Exp Med. 2021;218(11).
9. Hidano S, Randall LM, Dawson L, Dietrich HK, Konradt C, Klover PJ, et al. STAT1 Signaling in Astrocytes Is Essential for Control of Infection in the Central Nervous System. Mbio. 2016;7(6).
10. Matta SK, Rinkenberger N, Dunay IR, Sibley LD. Toxoplasma gondii infection and its implications within the central nervous system. Nature Reviews Microbiology. 2021.
11. Koblansky AA, Jankovic D, Oh H, Hieny S, Sungnak W, Mathur R, et al. Recognition of profilin by Toll-like receptor 12 is critical for host resistance to Toxoplasma gondii. Immunity. 2013;38(1):119-30.
12. Scanga CA, Aliberti J, Jankovic D, Tilloy F, Bennouna S, Denkers EY, et al. Cutting edge: MyD88 is required for resistance to Toxoplasma gondii infection and regulates parasite-induced IL-12 production by dendritic cells. J Immunol. 2002;168(12):5997-6001.
13. Yarovinsky F. Innate immunity to Toxoplasma gondii infection. Nature Reviews Immunology. 2014;14(2):109-21.
14. Yarovinsky F, Zhang D, Andersen JF, Bannenberg GL, Serhan CN, Hayden MS, et al. TLR11 Activation of Dendritic Cells by a Protozoan Profilin-Like Protein. Science. 2005;308(5728):1626-9.
15. Gazzinelli RT, Hieny S, Wynn TA, Wolf S, Sher A. Interleukin 12 is required for the T-lymphocyte-independent induction of interferon gamma by an intracellular parasite and induces resistance in T-cell-deficient hosts. Proc Natl Acad Sci U S A. 1993;90(13):6115-9.
16. Gazzinelli RT, Wysocka M, Hayashi S, Denkers EY, Hieny S, Caspar P, et al. Parasite-induced IL-12 stimulates early IFN-gamma synthesis and resistance during acute infection with Toxoplasma gondii. The Journal of Immunology. 1994;153(6):2533-43.
17. Khan IA, Matsuura T, Kasper LH. Interleukin-12 enhances murine survival against acute toxoplasmosis. Infect Immun. 1994;62(5):1639-42.

18. Ewald SE, Chavarria-Smith J, Boothroyd JC, Adams JH. NLRP1 Is an Inflammasome Sensor for Toxoplasma gondii. Infect Immun. 2014;82(1):460-8.
19. Gorfu G, Cirelli KM, Melo MB, Mayer-Barber K, Crown D, Koller BH, et al. Dual role for inflammasome sensors NLRP1 and NLRP3 in murine resistance to Toxoplasma gondii. Mbio. 2014;5(1).
20. López-Yglesias AH, Camanzo E, Martin AT, Araujo AM, Yarovinsky F. TLR11-independent inflammasome activation is critical for CD4+ T cell-derived IFN-γ production and host resistance to Toxoplasma gondii. PLoS Pathog. 2019;15(6):e1007872.
21. Witola WH, Mui E, Hargrave A, Liu S, Hypolite M, Montpetit A, et al. NALP1 influences susceptibility to human congenital toxoplasmosis, proinflammatory cytokine response, and fate of Toxoplasma gondii-infected monocytic cells. Infect Immun. 2011;79(2):756-66.
22. Cavailles P, Flori P, Papapietro O, Bisanz C, Lagrange D, Pilloux L, et al. A Highly Conserved Toxo1 Haplotype Directs Resistance to Toxoplasmosis and Its Associated Caspase-1 Dependent Killing of Parasite and Host Macrophage. PLOS Pathogens. 2014;10(4):e1004005.
23. Safronova A, Araujo A, Camanzo ET, Moon TJ, Elliott MR, Beiting DP, et al. Alarmin S100A11 initiates a chemokine response to the human pathogen Toxoplasma gondii. Nature immunology. 2019;20(1):64-72.
24. Batista SJ, Still KM, Johanson D, Thompson JA, O'Brien CA, Lukens JR, et al. Gasdermin-D-dependent IL-1α release from microglia promotes protective immunity during chronic Toxoplasma gondii infection. Nat Commun. 2020;11(1):3687.
25. Lees MP, Fuller SJ, McLeod R, Boulter NR, Miller CM, Zakrzewski AM, et al. P2X7 receptor-mediated killing of an intracellular parasite, Toxoplasma gondii, by human and murine macrophages. J Immunol. 2010;184(12):7040-6.
26. Pandori WJ, Lima TS, Mallya S, Kao TH, Gov L, Lodoen MB. Toxoplasma gondii activates a Syk-CARD9-NF-κB signaling axis and gasdermin D-independent release of IL-1β during infection of primary human monocytes. PLOS Pathogens. 2019;15(8):e1007923.
27. Wang Y, Cirelli KM, Barros PDC, Sangaré LO, Butty V, Hassan MA, et al. Three Toxoplasma gondii Dense Granule Proteins Are Required for Induction of Lewis Rat Macrophage Pyroptosis. Mbio. 2019;10(1):e02388-18.
28. Still KM, Batista SJ, O'Brien CA, Oyesola OO, Früh SP, Webb LM, et al. Astrocytes promote a protective immune response to brain Toxoplasma gondii infection via IL-33-ST2 signaling. PLOS Pathogens. 2020;16(10):e1009027.
29. Clark JT, Weizman OE, Aldridge DL, Shallberg LA, Eberhard J, Lanzar Z, et al. IL-18BP mediates the balance between protective and pathological immune responses to Toxoplasma gondii. Cell Rep. 2023;42(3):112147.
30. Rauch I, Deets KA, Ji DX, von Moltke J, Tenthorey JL, Lee AY, et al. NAIP-NLRC4 Inflammasomes Coordinate Intestinal Epithelial Cell Expulsion with Eicosanoid and IL-18 Release via Activation of Caspase-1 and -8. Immunity. 2017;46(4):649-59.
31. Sims JE, Smith DE. The IL-1 family: regulators of immunity. Nature Reviews Immunology. 2010;10(2):89-102.
32. Yona S, Kim K-W, Wolf Y, Mildner A, Varol D, Breker M, et al. Fate Mapping Reveals Origins and Dynamics of Monocytes and Tissue Macrophages under Homeostasis. Immunity. 2013;38(1):79-91.
33. Case CL, Kohler LJ, Lima JB, Strowig T, de Zoete MR, Flavell RA, et al. Caspase-11 stimulates rapid flagellin-independent pyroptosis in response to Legionella pneumophila. Proc Natl Acad Sci U S A. 2013;110(5):1851-6.

34. Jung S, Aliberti J, Graemmel P, Sunshine MJ, Kreutzberg GW, Sher A, et al. Analysis of fractalkine receptor CX(3)CR1 function by targeted deletion and green fluorescent protein reporter gene insertion. Mol Cell Biol. 2000;20(11):4106-14.
35. Cirelli KM, Gorfu G, Hassan MA, Printz M, Crown D, Leppla SH, et al. Inflammasome Sensor NLRP1 Controls Rat Macrophage Susceptibility to Toxoplasma gondii. PLOS Pathogens. 2014;10(3):e1003927.
36. Bliss SK, Gavrilescu LC, Alcaraz A, Denkers EY. Neutrophil depletion during Toxoplasma gondii infection leads to impaired immunity and lethal systemic pathology. Infect Immun. 2001;69(8):4898-905.
37. Miranda FJB, Rocha BC, Pereira MCA, Pereira LMN, de Souza EHM, Marino AP, et al. Toxoplasma gondii-Induced Neutrophil Extracellular Traps Amplify the Innate and Adaptive Response. Mbio. 2021;12(5):e0130721.
38. Dunay IR, Fuchs A, Sibley LD. Inflammatory Monocytes but Not Neutrophils Are Necessary To Control Infection with Toxoplasma gondii in Mice. Infect Immun. 2010;78(4):1564-70.
39. Ryffel B, Huang F, Robinet P, Panek C, Couillin I, Erard F, et al. Corrigendum: Blockade of IL-33R/ST2 Signaling Attenuates Toxoplasma gondii Ileitis Depending on IL-22 Expression. Frontiers in Immunology. 2020;11.
40. Cayrol C, Girard JP. The IL-1-like cytokine IL-33 is inactivated after maturation by caspase-1. Proc Natl Acad Sci U S A. 2009;106(22):9021-6.
41. Alvarez F, Fritz JH, Piccirillo CA. Pleiotropic Effects of IL-33 on CD4+ T Cell Differentiation and Effector Functions. Frontiers in Immunology. 2019;10.
42. Chen W, Chen S, Yan C, Zhang Y, Zhang R, Chen M, et al. Allergen protease-activated stress granule assembly and gasdermin D fragmentation control interleukin-33 secretion. Nature Immunology. 2022;23(7):1021-30.
43. Yamagishi R, Kamachi F, Nakamura M, Yamazaki S, Kamiya T, Takasugi M, et al. Gasdermin D-mediated release of IL-33 from senescent hepatic stellate cells promotes obesity-associated hepatocellular carcinoma. Sci Immunol. 2022;7(72):eabl7209.
44. Yoshimoto T, Takeda K, Tanaka T, Ohkusu K, Kashiwamura S, Okamura H, et al. IL-12 up-regulates IL-18 receptor expression on T cells, Th1 cells, and B cells: synergism with IL-18 for IFN-gamma production. J Immunol. 1998;161(7):3400-7.
45. Cai G, Kastelein R, Hunter CA. Interleukin-18 (IL-18) enhances innate IL-12-mediated resistance to Toxoplasma gondii. Infect Immun. 2000;68(12):6932-8.
46. Kupz A, Pai S, Giacomin PR, Whan JA, Walker RA, Hammoudi P-M, et al. Treatment of mice with S4B6 IL-2 complex prevents lethal toxoplasmosis via IL-12- and IL-18-dependent interferon-gamma production by non-CD4 immune cells. Scientific Reports. 2020;10(1):13115.
47. Christian DA, Koshy AA, Reuter MA, Betts MR, Boothroyd JC, Hunter CA. Use of Transgenic Parasites and Host Reporters To Dissect Events That Promote Interleukin-12 Production during Toxoplasmosis. Infect Immun. 2014;82(10):4056-67.
48. Fisch D, Bando H, Clough B, Hornung V, Yamamoto M, Shenoy AR, et al. Human GBP1 is a microbe-specific gatekeeper of macrophage apoptosis and pyroptosis. The EMBO Journal. 2019;38(13):e100926.
49. Moreira-Souza ACA, Almeida-da-Silva CLC, Rangel TP, Rocha GdC, Bellio M, Zamboni DS, et al. The P2X7 Receptor Mediates Toxoplasma gondii Control in Macrophages through Canonical NLRP3 Inflammasome Activation and Reactive Oxygen Species Production. Frontiers in Immunology. 2017;8.

631 50. Gai K, Okondo MC, Rao SD, Chui AJ, Ball DP, Johnson DC, et al. DPP8/9 inhibitors are
632 universal activators of functional NLRP1 alleles. Cell Death & Disease. 2019;10(8):587.
633 51. Swanson KV, Deng M, Ting JPY. The NLRP3 inflammasome: molecular activation and
634 regulation to therapeutics. Nature Reviews Immunology. 2019;19(8):477-89.
635 52. Fisch D, Clough B, Domart M-C, Encheva V, Bando H, Snijders AP, et al. Human GBP1
636 Differentially Targets Salmonella and Toxoplasma to License
637 Recognition of Microbial Ligands and Caspase-Mediated Death. Cell Reports. 2020;32(6).
638 53. Dinarello CA. Overview of the IL-1 family in innate inflammation and acquired immunity.
639 Immunol Rev. 2018;281(1):8-27.
640 54. Kuida K, Lippke JA, Ku G, Harding MW, Livingston DJ, Su MS, et al. Altered cytokine
641 export and apoptosis in mice deficient in interleukin-1 beta converting enzyme. Science.
642 1995;267(5206):2000-3.
643 55. Takeda K, Tsutsui H, Yoshimoto T, Adachi O, Yoshida N, Kishimoto T, et al. Defective NK
644 cell activity and Th1 response in IL-18-deficient mice. Immunity. 1998;8(3):383-90.
645 56. Cullinan EB, Kwee L, Nunes P, Shuster DJ, Ju G, McIntyre KW, et al. IL-1 receptor
646 accessory protein is an essential component of the IL-1 receptor. J Immunol. 1998;161(10):5614-
647 20.
648 57. Homan WL, Vercammen M, De Braekeleer J, Verschueren H. Identification of a 200- to
649 300-fold repetitive 529 bp DNA fragment in Toxoplasma gondii, and its use for diagnostic and
650 quantitative PCR. Int J Parasitol. 2000;30(1):69-75.
651 58. Livak KJ, Schmittgen TD. Analysis of relative gene expression data using real-time
652 quantitative PCR and the 2(-Delta Delta C(T)) Method. Methods. 2001;25(4):402-8.
653 59. Bates D, Mächler M, Bolker B, Walker S. Fitting Linear Mixed-Effects Models Using
654 lme4. Journal of Statistical Software. 2015;67(1):1 - 48.
655 60. Motulsky HJ, Brown RE. Detecting outliers when fitting data with nonlinear regression -
656 a new method based on robust nonlinear regression and the false discovery rate. BMC
657 Bioinformatics. 2006;7:123.

658

659

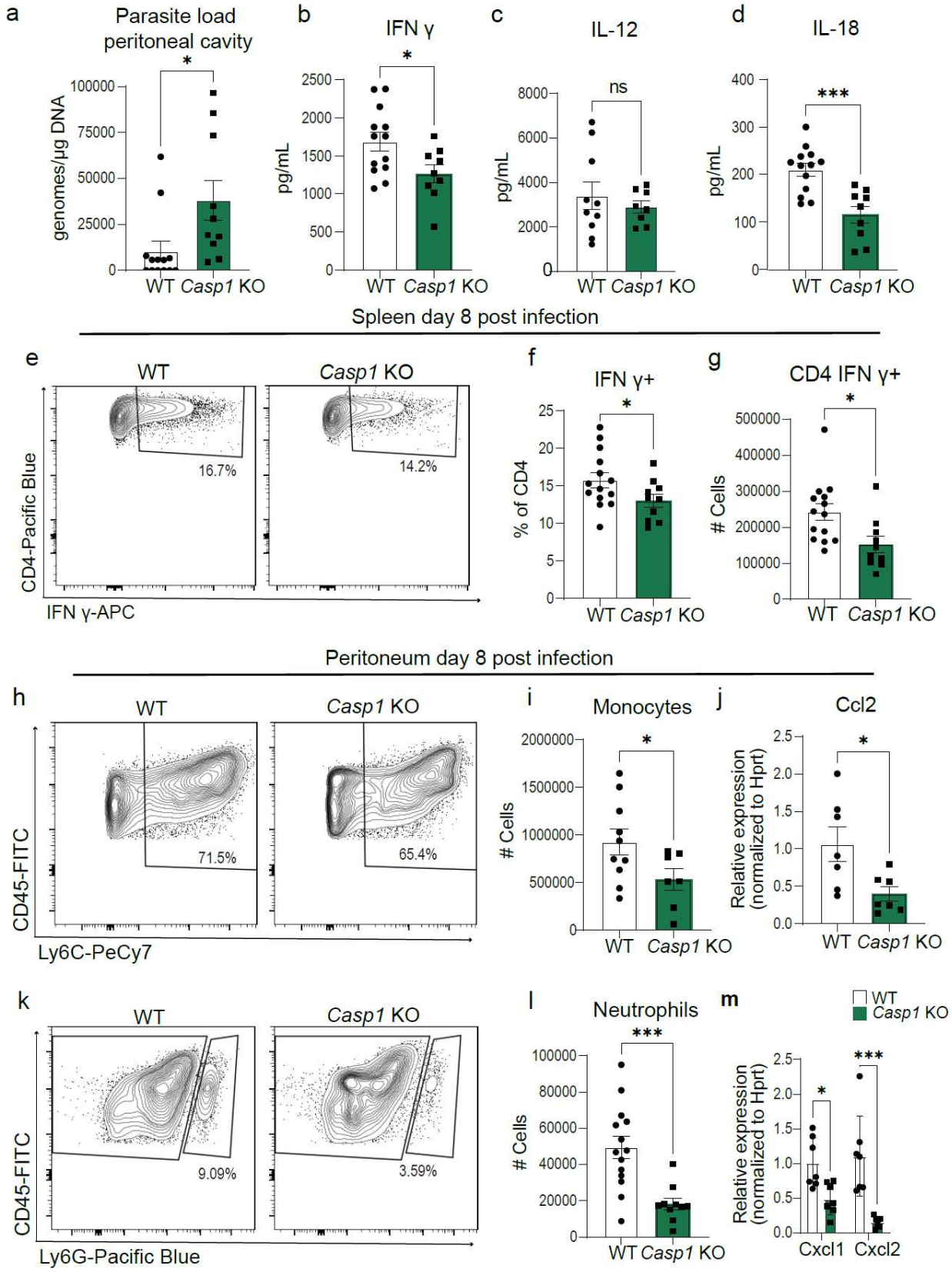

Figure 1. *Caspase-1 mediates innate and adaptive immune responses to T. gondii.*

(a) qPCR analysis of *T. gondii* parasite load 8 days post-infection (8 dpi) in the peritoneum of wildtype WT C57BL/6 (n=13) and *Casp1* Knockout (*Casp1* KO) (n=10) mice, three experiments. (b-d) Serum cytokine levels 8 dpi, three experiments for (b) IFN-γ: WT (n=13), *Casp1* KO (n=9); (c) IL-12: WT (n=10), *Casp1* KO (n=8); and (d) IL-18: WT (n=13), *Casp1* KO (n=9). (e-g) Flow cytometry of $CD3^+$ $CD4^+$ IFN-γ^+ T cells in spleen at 8 dpi, three experiments, WT (n=14), *Casp1* KO (n=10). (e) Representative flow cytometry plot. (f) Frequency of $CD4^+$ T cells IFN-γ^+. (g) Number of $CD4^+$ T cells producing IFN-γ. (h) Representative flow cytometry plots of $CD45^+$ $CD11b^+$ $Ly6C^+$ monocytes in the peritoneum 8dpi. (i) Number of $CD45^+$ $CD11b^+$ $Ly6C^+$ monocytes in WT (n=10), *Casp1* KO (n=7), two experiments. (j) RT-qPCR analysis of peritoneal Ccl2 expression in WT (n=7) and *Casp1* KO (n=7), two experiments. (k) Representative flow cytometry plot of $CD45^+$ $CD11b^+$ $Ly6G^+$ neutrophils in the peritoneum at 8 dpi. (l) Number of $CD45^+$ $CD11b^+$ $Ly6G^+$ neutrophils in WT (n=15), *Casp1* KO (n=9), three experiments. (m) RT-qPCR analysis of peritoneal Cxcl1 and Cxcl2 expression in WT (n=7) and *Casp1* KO (n=7), two experiments. Data are mean ± s.e.m., ns= not significant, * $p < 0.05$, *** $p < 0.001$ by randomized-block ANOVA and post-hoc Tukey test (a-d,f-g,i-j, and l-m).

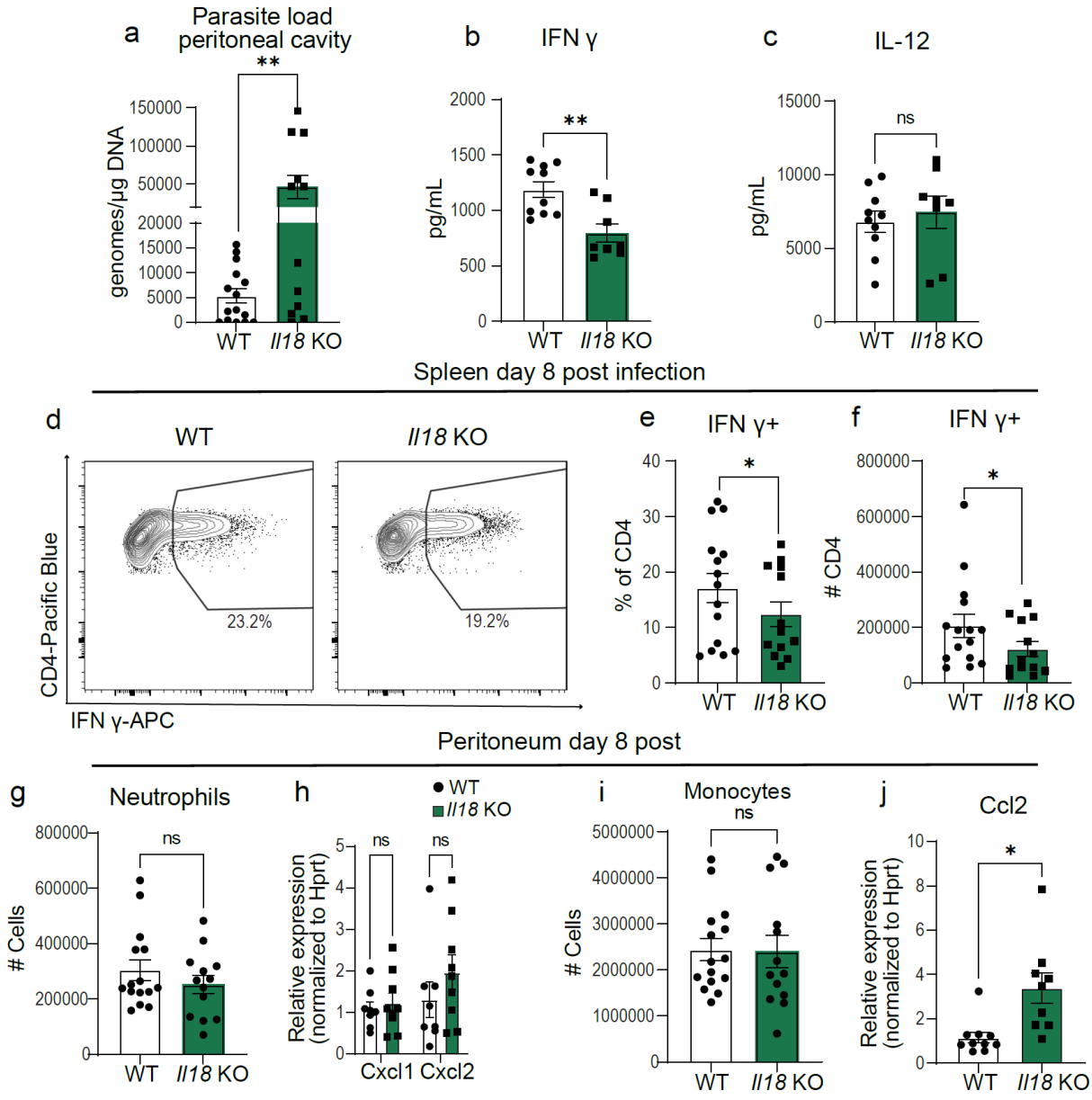

Figure 2. IL-18 promotes CD4⁺ T cell IFN-γ production but is dispensable for myeloid cell recruitment to the initial site of infection.

(a) qPCR analysis of *T. gondii* parasite load 8 days post-infection (8 dpi) in the peritoneum of wildtype (WT) C57BL/6 (n=15) and *Il18* KO (n=12) mice, three experiments. (b,c) Serum cytokine levels 8 dpi, two experiments for (b) IFN-γ: WT (n=10), *Il18* KO (n=8); (c) IL-12: WT (n=10), *Il18* KO (n=8). (d-f) Flow cytometry of $CD3^+$ $CD4^+$ IFN-γ^+ T cells in spleen at 8 dpi, three

685 experiments, WT (n=15), *Il18* KO (n=13). (d) Representative flow cytometry plot. (e) Frequency
686 of $CD4^+$ T cells IFN-γ^+. (f) Number of $CD4^+$ T cells producing IFN-γ. (g) Number of $CD45^+$
687 $CD11b^+$ $Ly6G^+$ neutrophils in WT (n=15), *Il18* KO (n=13), three experiments. (h) RT-qPCR
688 analysis of peritoneal Cxcl1 and Cxcl2 expression in WT (n=7) and *Il-18* KO (n=9), two
689 experiments. (i) Number of $CD45^+$ $CD11b^+$ $Ly6C^+$ monocytes in WT (n=15), *Il18* KO (n=13), three
690 experiments. (j) RT-qPCR analysis of peritoneal Ccl2 expression in WT (n=10) and *Il18* KO (n=9),
691 two experiments. Data are mean ± s.e.m., ns= not significant, * $p < 0.05$,** $p < 0.01$ by
692 randomized-block ANOVA and post-hoc Tukey test (a-c and e-j).

693

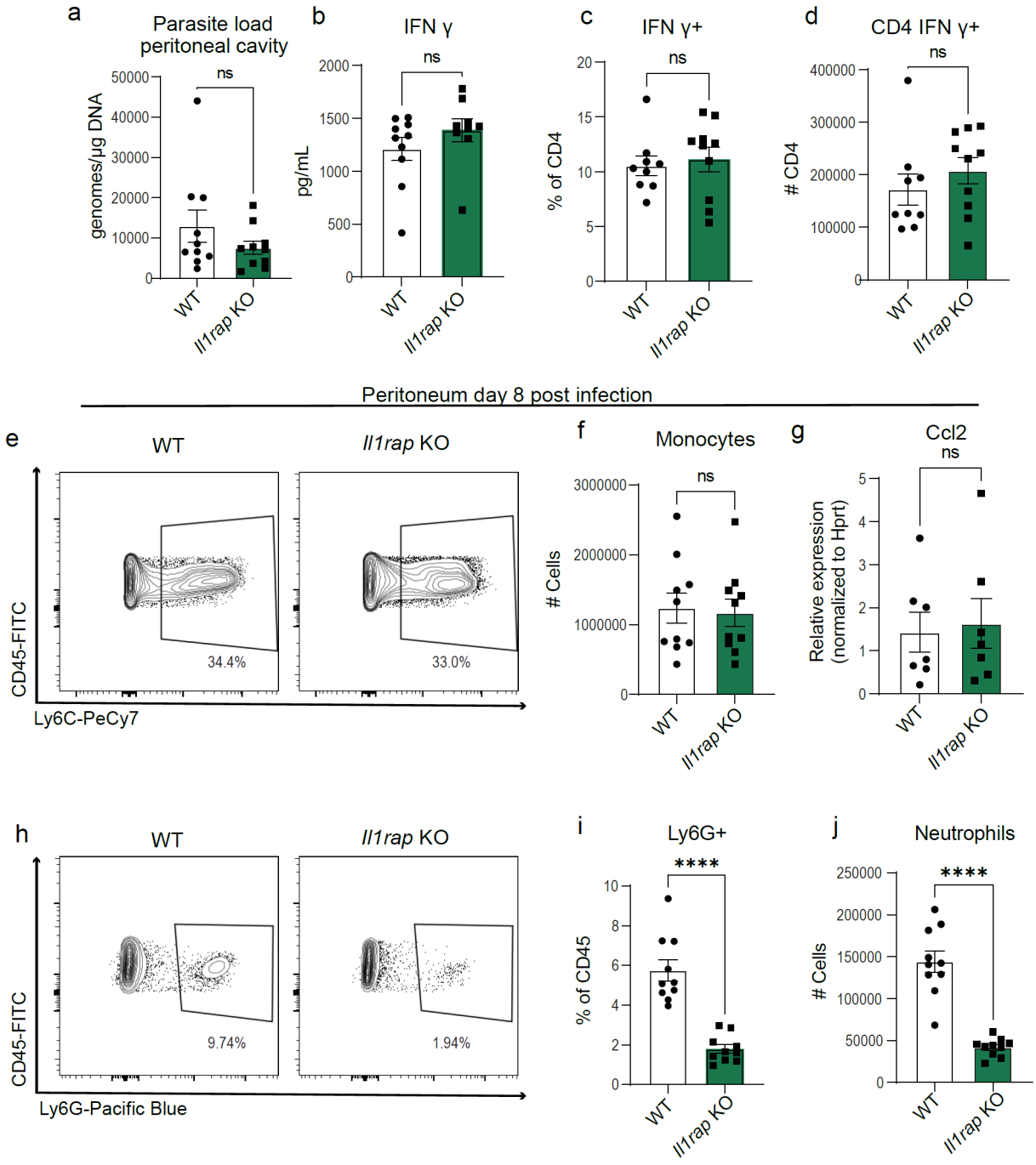

694

695 *Figure 3. IL-1RAP signaling mediates neutrophil recruitment to the sight of infection but is*

696 *dispensable for parasite control during acute T. gondii infection.*

697 (a) qPCR analysis of *T. gondii* parasite load 8 days post-infection (8 dpi) in the peritoneum of

698 *Il1rap* KO and wildtype (WT) mice, C57BL/6 (*n*=10) and *Il1rap* KO (*n*=10) mice, two

699 experiments. (b) Serum cytokine levels 8 dpi, two experiments for IFN-γ: WT (*n*=10), *Il1rap* KO
700 (*n*=10). (c-d) Flow cytometry of $CD3^+$ $CD4^+$ IFN-γ^+ T cells in spleen at 8 dpi, two experiments,
701 WT (*n*=9), *Il1rap* KO (*n*=10). (c) Frequency of $CD4^+$ T cells IFN-γ^+. (d) Number of $CD4^+$ T cells
702 producing IFN-γ. (e) Representative flow cytometry plots of $CD45^+$ $CD11b^+$ $Ly6C^+$ monocytes in
703 the peritoneum at 8dpi. (f) Number of $CD45^+$ $CD11b^+$ $Ly6C^+$ monocytes in WT (*n*=10), *Il1rap* KO
704 (*n*=10), two experiments. (j) RT-qPCR analysis of peritoneal Ccl2 expression in WT (*n*=7) and
705 *Il1rap* KO (*n*=7), two experiments. (h) Representative flow cytometry plot of $CD45^+$ $CD11b^+$
706 $Ly6G^+$ neutrophils in the peritoneum at 8 dpi. (i) Frequency and (j) Number of $CD45^+$ $CD11b^+$
707 $Ly6G^+$ neutrophils in WT (n=10) and *Il1rap* KO (n=10), two experiments. Data are mean ± s.e.m.,
708 ns = not significant, **** $p < 0.0001$, randomized-block ANOVA and post-hoc Tukey test (a-d,f-
709 g, and i-j).

710

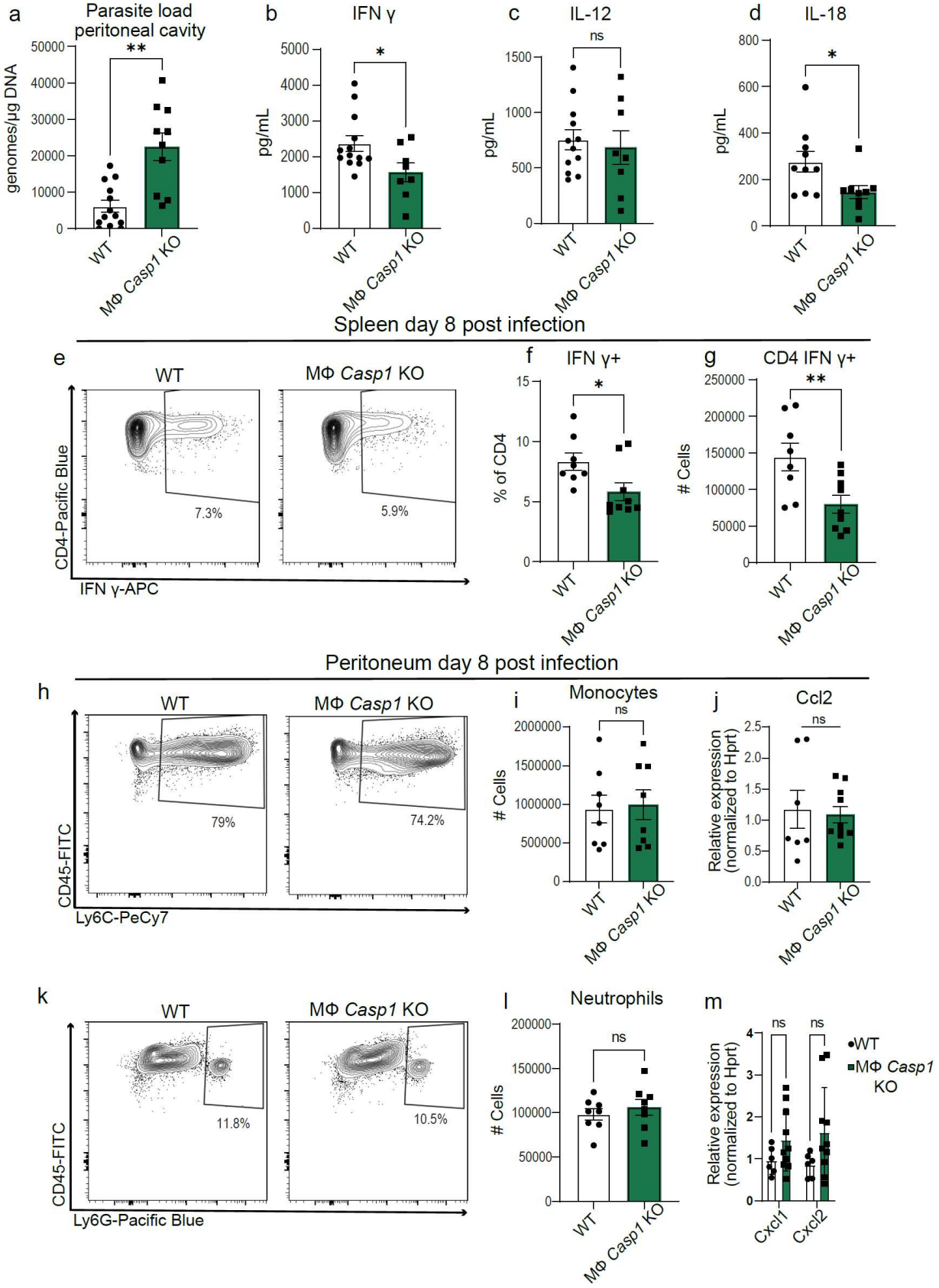

Figure 4. *Caspase-1 in Cx3cr1-expressing cells is necessary for parasite control and optimal CD4$^+$T cell production of IFN-γ*

(a) qPCR analysis of *T. gondii* parasite load 8 days post-infection (8 dpi) in the peritoneum of *Cx3cr1*$^{+/+}$ *Caspase 1*$^{fl/fl}$ (WT) (n=13) and *Cx3cr1*$^{Cre/+}$ *Caspase 1*$^{fl/fl}$ (MΦ *Casp1* KO) (n=10) mice, three experiments. (b-d) Serum cytokine levels 8 dpi, three experiments for (b) IFN-γ: WT (n=13), MΦ *Casp1* KO (n=8); (c) IL-12: WT (n=12), MΦ *Casp1* KO (n=8); and (d) IL-18: WT (n=10), MΦ *Casp1* KO (n=9). (e-g) Flow cytometry of CD3$^+$ CD4$^+$ IFN-γ$^+$ T cells in spleen at 8 dpi, two experiments, WT (n=8), MΦ *Casp1* KO (n=9). (e) Representative flow cytometry plot. (f) Frequency of IFN-γ-producing CD4$^+$ T cells (g) Number of CD4$^+$ T cells producing IFN-γ. (h) Representative flow cytometry plots of CD45$^+$ CD11b$^+$ Ly6C$^+$ monocytes in the peritoneum 8 dpi. (i) Number of CD45$^+$ CD11b$^+$ Ly6C$^+$ monocytes in WT (n=8) and MΦ *Casp1* KO (n=8), two experiments. (j) RT-qPCR analysis of peritoneal Ccl2 expression in WT (n=7) and MΦ *Casp1* KO (n=10), two experiments. (k) Representative flow cytometry plot of CD45$^+$ CD11b$^+$ Ly6G$^+$ neutrophils in the peritoneum at 8 dpi. (l) Number of CD45$^+$ CD11b$^+$ Ly6G$^+$ neutrophils in WT (n=8), MΦ *Casp1* KO (n=9), two experiments. (m) RT-qPCR analysis of peritoneal Cxcl1 and Cxcl2 expression in WT (n=6) and MΦ *Casp1* KO (n=10), two experiments. Data are mean ± s.e.m. ns= not significant, * $p < 0.05$, ** $p < 0.01$ by randomized-block ANOVA and post-hoc Tukey test (a-d, f-g, i-j, and l-m).

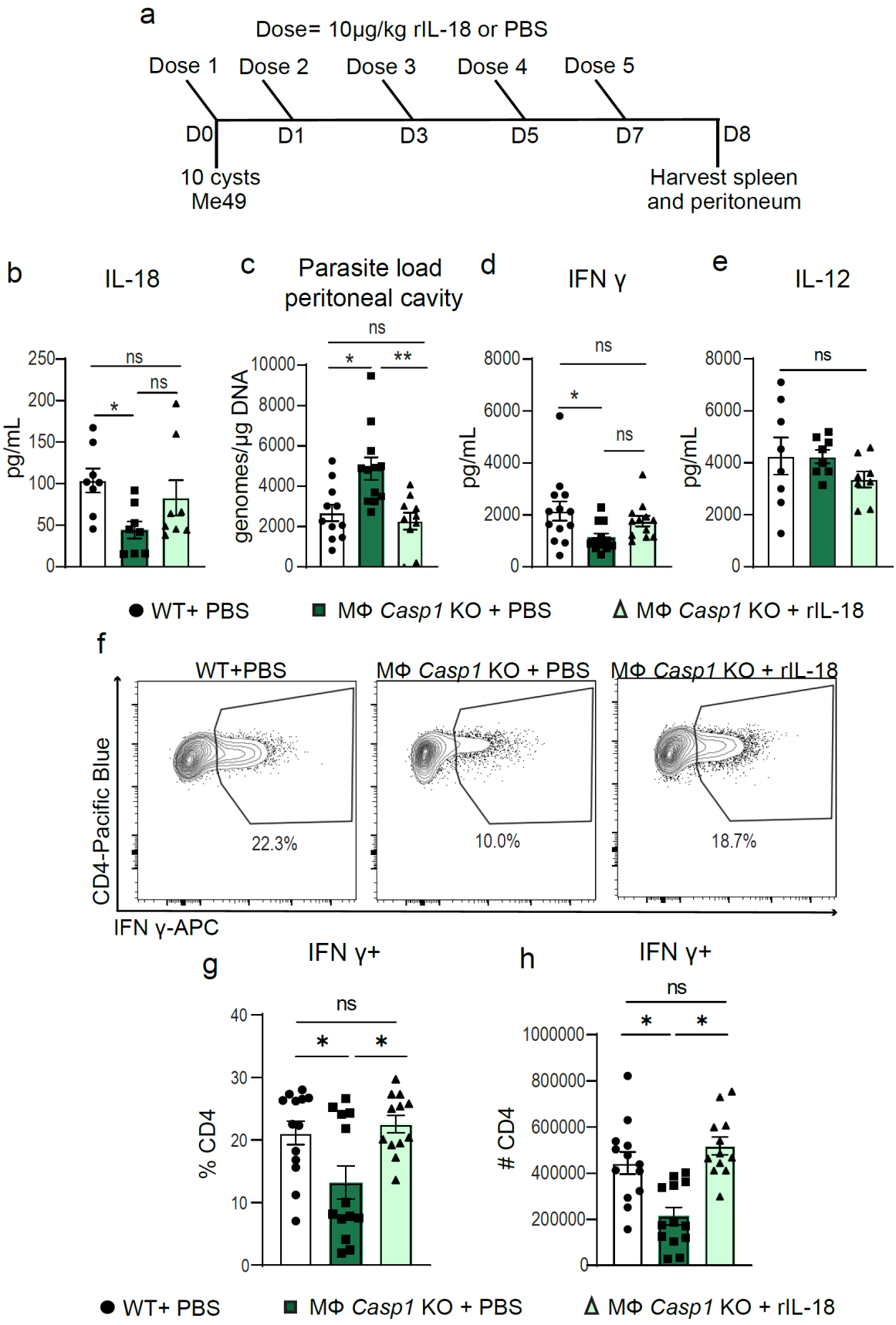

Figure 5. *Recombinant IL-18 administration rescues CD4$^+$ T cell IFN-γ production and parasite control in macrophage caspase-1 deficient mice.*

(a) Schematic of experimental design. (b) Serum cytokine levels of IL-18, two experiments, WT + PBS (*n*=8), MΦ *Casp1* KO + PBS (*n*=8), and MΦ *Casp1* KO + rIL-18 (*n*=8). (c) qPCR analysis of parasite load in peritoneal cavity, three experiments, WT + PBS (*n*=11), MΦ *Casp1* KO + PBS (*n*=12), and MΦ *Casp1* KO + rIL-18 (*n*=10). (d) Serum cytokine levels of IFN-γ, three experiments, WT + PBS (*n*=13), MΦ *Casp1* KO + PBS (*n*=12), and MΦ *Casp1* KO + rIL-18 (*n*=12). (e) Serum cytokine levels of IL-12, two experiments, WT + PBS (*n*=8), MΦ *Casp1* KO + PBS (*n*=8), and MΦ *Casp1* KO + rIL-18 (*n*=8). (f-h) Flow cytometry of CD3$^+$ CD4$^+$ IFN-γ$^+$ T cells in spleen at 8 dpi, three experiments, WT + PBS (n=13), MΦ *Casp1* KO + PBS (n=12), and MΦ *Casp1* KO + rIL-18 (n=12) . (f) Representative flow cytometry plot. (g) Frequency of CD4$^+$ T cells IFN-γ$^+$. (h) Number of CD4$^+$ T cells producing IFN-γ. Data are presented as mean ± s.e.m., ns= not significant, * $p < 0.05$, ** $p < 0.01$ by randomized-block ANOVA and post-hoc Tukey test (b-e, g-h).

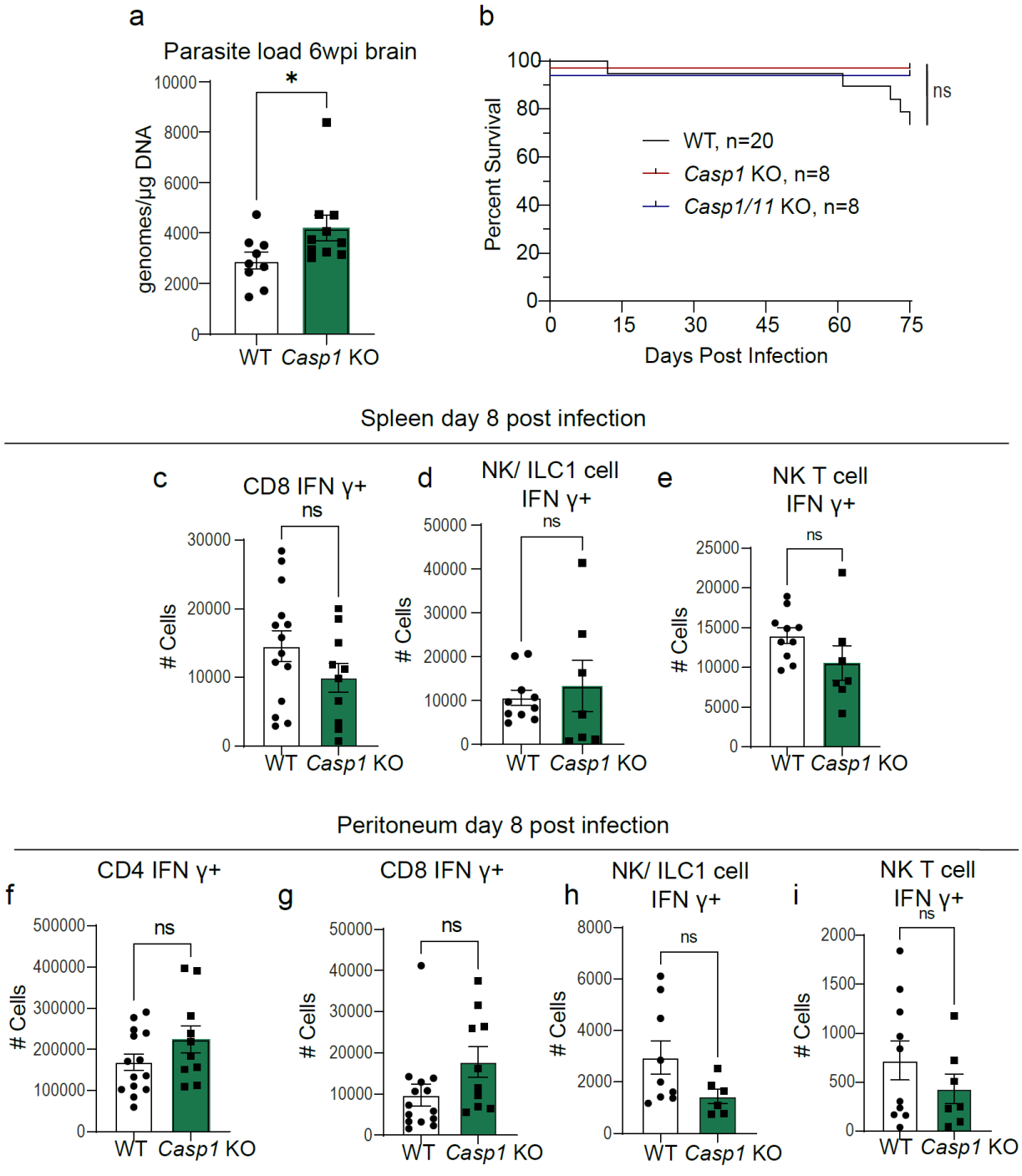

747

748 Supplemental Figure 1. *Parasite load during chronic infection, survival, and acute cytokine*

749 *production in Casp1 KO mice.*

(a) qPCR analysis of *T. gondii* parasite load 6 weeks post-infection (6wpi) in the brain of wildtype WT C57BL/6 (n=9) and *Casp1* KO (n=10) mice, two experiments. (b) Ethical end-point curve WT (n=20), *Casp1* KO (n=8), and *Casp1/11* KO (n=8). (c) Flow cytometry of $CD3^+$ $CD8^+$ IFN-γ^+ T cells in spleen at 8 dpi, three experiments, WT (n=14) and *Casp1* KO (n=10). (d) Flow cytometry of $CD3^-$ $NK1.1^+$ $T\text{-}bet^+$ IFN-γ^+ NK cells and or ILC1 cells in spleen at 8 dpi, two experiments WT (n=10), *Casp1* KO (n=7). (e) Flow cytometry of $CD3^+$ $NK1.1^+$ $T\text{-}bet^+$ IFN-γ^+ NK T cells in spleen at 8 dpi, two experiments WT (n=10), *Casp1* KO (n=7). (f-g) Flow cytometry of $CD3^+$ (f) $CD4^+$, and (g) $CD8^+$ IFN-γ^+ T cells in peritoneum at 8 dpi, three experiments, WT (n=14), *Casp1* KO (n=10). (h) Flow cytometry of $CD3^-$ $NK1.1^+$ $T\text{-}bet^+$ IFN-γ^+ NK cells and or ILC1 cells in peritoneum at 8 dpi, two experiments WT (n=9), *Casp1* KO (n=6), one outlier removed from WT and one from *Casp1* KO. (i) Flow cytometry of $CD3^+$ $NK1.1^+$ $T\text{-}bet^+$ IFN-γ^+ NK T cells in peritoneum at 8 dpi, two experiments WT (n=10), *Casp1* KO (n=7). Data are presented as mean ± s.e.m., ns= not significant, * $p < 0.05$ by randomized-block ANOVA and post-hoc Tukey test (a,c-i) or log-rank (Mantel Cox) test (b).

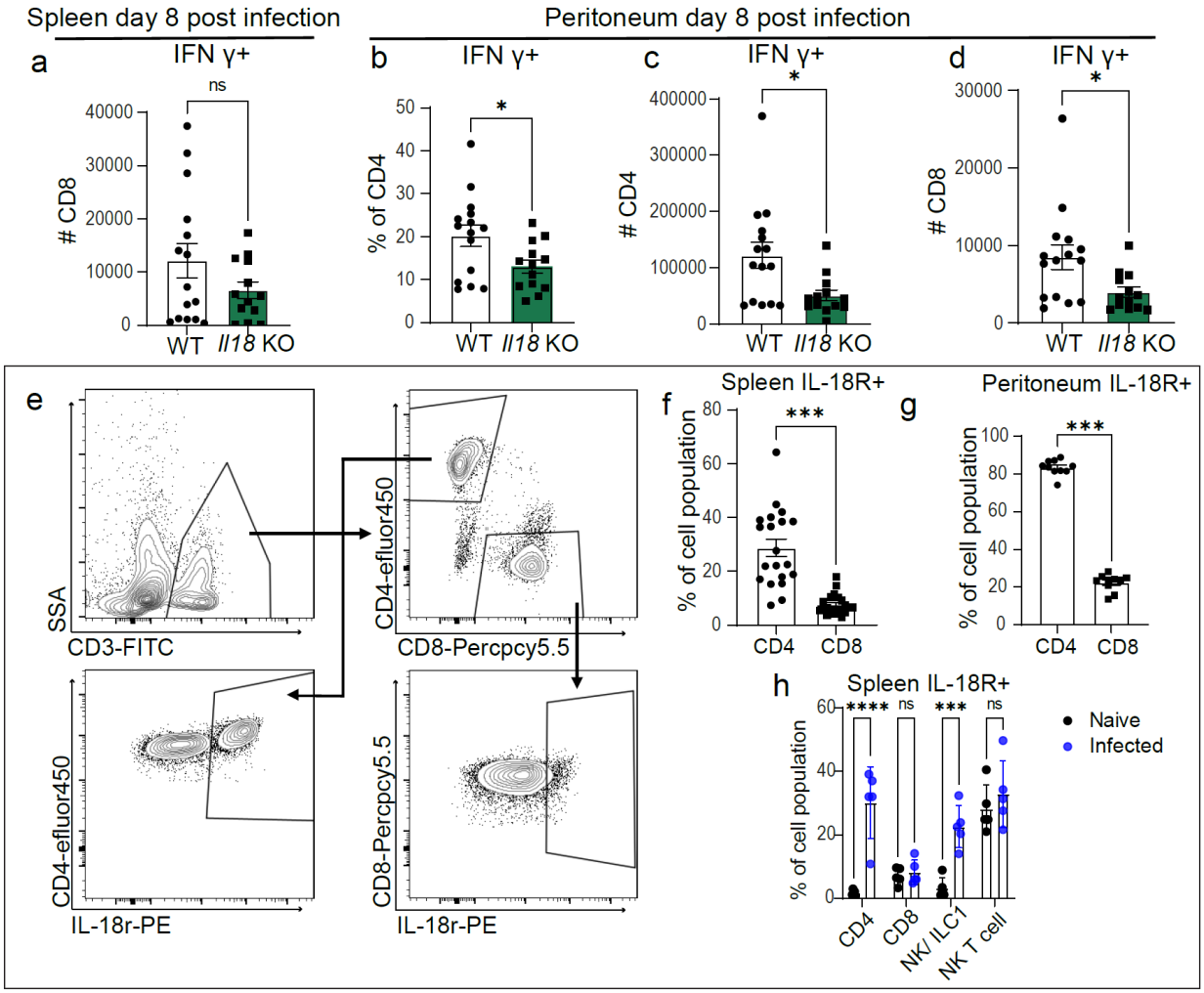

Supplemental Figure 2. *Cytokine production in Il18 KO mice and IL-18R expression*

(a) Flow cytometry of $CD3^+$ $CD8^+$ IFN-γ^+ T cells in spleens 8 dpi, three experiments, WT (*n*=15) and *Il18* KO (*n*=13). (b,c) Flow cytometry analysis of frequency (b) and number (c) of $CD3^+$ $CD4^+$ IFN-γ^+ T cells in peritoneum 8 dpi, three experiments, WT (*n*=15) and *Il18* KO (*n*=13). (d) Flow cytometry number of $CD3^+$ $CD8^+$ IFN-γ^+ T cells in peritoneum 8 dpi, three experiments, WT (*n*=15) and *Il18* KO (*n*=13). (e) Flow-gating strategy for IL-18 receptor (IL-18R) expression in $CD4^+$ and $CD8^+$ T cells. (f) Flow cytometry analysis of splenic $CD3^+$ $CD4^+$ and $CD8^+$ T cells IL-18R expression, two experiments, (*n*=20). (g) Flow cytometry analysis of peritoneal $CD3^+$ $CD4^+$

784 and $CD8^+$ T cell IL-18R expression, one experiment, (n=10). (h) Flow cytometry analysis of
785 splenic $CD3^+$ $CD4^+$ and $CD8^+$ T cells, NK cells and or ILC1 cells (CD3- NK1.1+ Tbet+) and NK
786 T cells (CD3+ NK1.1+ Tbet+) IL-18R expression in naïve (n=5) and infected mice (n=5). Data
787 are presented as mean ± s.e.m., ns= not significant, * $p < 0.05$, *** $p < 0.001$, **** $p < 0.0001$ by
788 randomized-block ANOVA and post-hoc Tukey test (a-d,f) or Student's t-test (g-h).

789

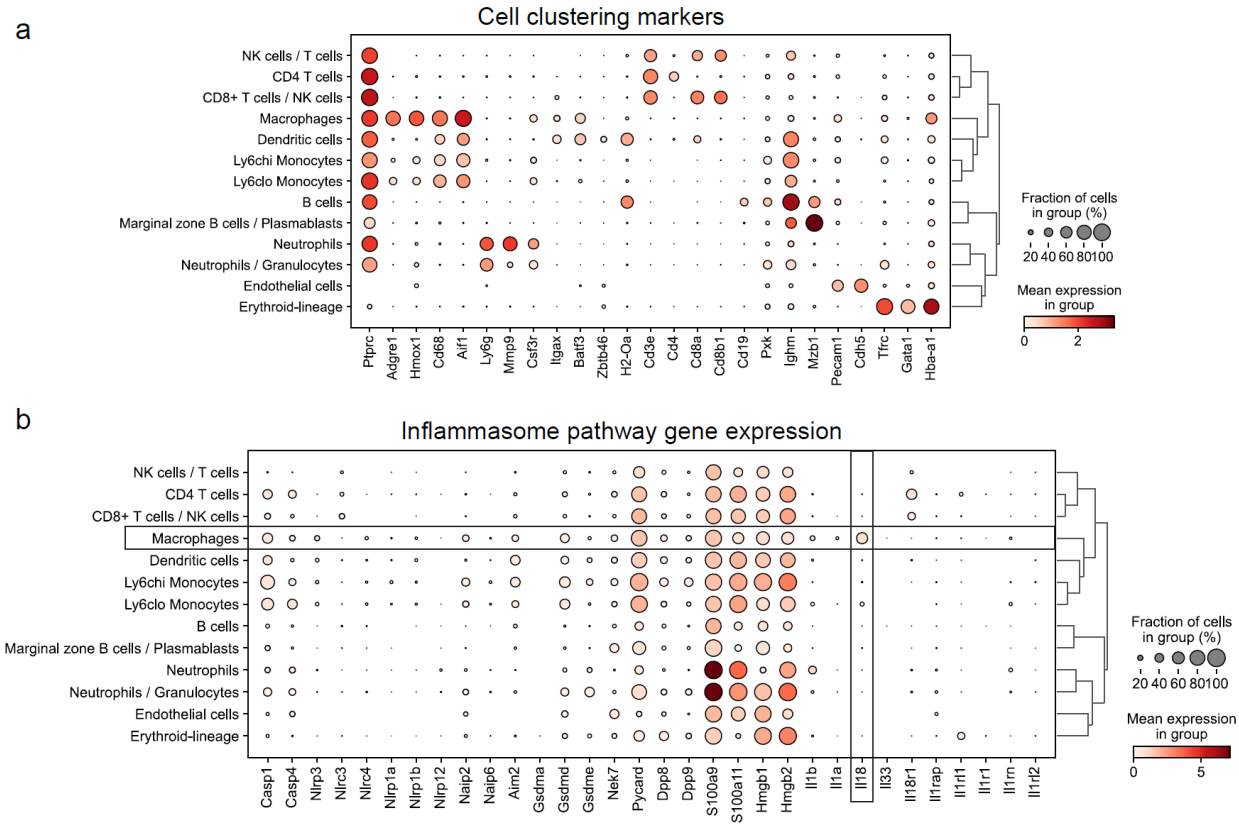

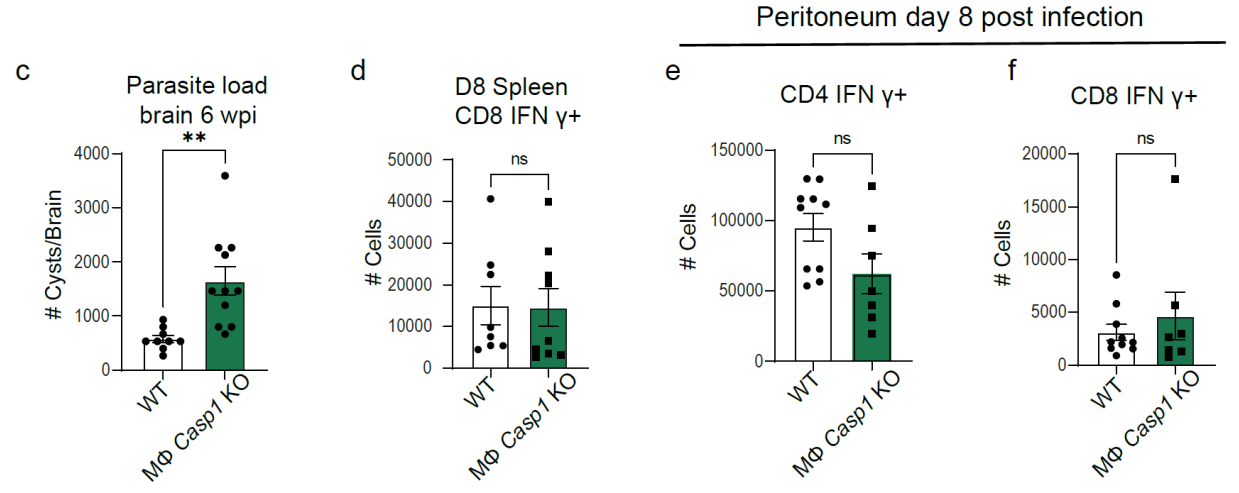

792 Supplemental Figure 3. *Expression of cell death-related genes using single-cell RNAseq and*
793 *parasite burden and cytokine production in macrophage Casp1 KO mice*

794 (a-b) Analysis of single cell RNA sequencing of the spleen on day 14 post-infection from (29)(a)
795 Cell cluster segmentation markers (b) Cell type expression of manually selected inflammasome
796 and cytokine related genes. (c) Cyst counts of *T. gondii* parasite load 6 weeks post-infection (6wpi)
797 in the brain of wildtype WT (n=9) and MΦ *Casp1* KO (n=11) mice, two experiments. (d) Flow
798 cytometry of $CD3^+$ $CD8^+$ IFN-γ^+ T cells in spleen at 8 dpi, two experiments, WT (n=8) and MΦ
799 *Casp1* KO (n=9). (e-f) Flow cytometry of $CD3^+$ (e) $CD4^+$ (f) $CD8^+$ IFN-γ^+ T cells in peritoneum
800 at 8 dpi, two experiments, WT (n=10) and MΦ *Casp1* KO (n=7). Data are presented as
801 mean ± s.e.m., ns= not significant, ** $p < 0.01$ by randomized-block ANOVA and post-hoc Tukey
802 test (c-f).

803